J|A|C|S
COMMUNICATIONS

Published on Web 05/25/2006

Unique Crystal Morphologies of Glycine Grown from Octanoic Acid-in-Water Emulsions

Catherine E. Nicholson, Sharon J. Cooper,* and Matthew J. Jamieson

Department of Chemistry, University of Durham, South Road, Durham. DH1 3LE, United Kingdom

Received January 17, 2006; E-mail: sharon.cooper@durham.ac.uk

We have obtained both porous and dendritic, intricate morphology crystals of glycine by the novel and simple method of emulsion droplet adhesion. By using octanoic acid emulsified with nonionic surfactants, the adhesion of the emulsion droplets can be so strong that crystal growth often proceeds around the droplets, leading to their inclusion within the single crystals. Consequently, porous single crystals can be produced with the pore diameters (~10−25 μm) corresponding to the emulsion droplet sizes, see Figure 1a. The single crystal nature of the glycine is clearly shown by X-ray diffraction studies and the continuity of birefringence colors observed in the polarizing microscope. The highly curved growth fronts on the growing crystal (see Figure 1a, arrowed regions) arise from the partial inclusion of oil droplets, many of which become fully incorporated with further crystal growth (see Figure 1b).

The porous single crystals are obtained from a 21.5 wt % glycine aqueous phase, which is emulsified with 60 wt % octanoic acid and a 9 wt % nonionic surfactant mixture comprising 8:1 Span 20/Brij 30 or 8:1 Tween 20/Brij 30. The crystallization is induced by cooling from 25 to 20 °C. In situ X-ray diffraction of the growing crystals indicated that the β-polymorph grew predominantly in these emulsions, rather than the α-phase, which is expected at the pH of 5.5 found for these emulsions. This demonstrates that the nonionic surfactants were the nucleating agents, since the β-phase has previously been obtained within emulsion droplets stabilized with these surfactants.[1] The transformation of the β-polymorph to the more stable α-polymorph typically occurs readily in aqueous solution.[2] However, this effect was not observed in our systems presumably because the octanoic acid and surfactants adsorbed onto the crystals hinder the solvent-mediated polymorphic transformation.

On changing the oil phase to decane, no droplet adhesion occurred, and porous crystals were not obtained. However, the surfactant mixture still promoted the glycine β-polymorph. Droplet adhesion was also not observed on acidification of this system to a pH of 5.5, i.e. the same pH as in the octanoic acid emulsions, although on decreasing the pH further to ~3 a small proportion (<10%) of crystals showed a little porosity with typically ~3−4 droplets encapsulated within crystals of millimeter size. In all cases, the β-polymorph was obtained. The lack of γ-polymorph crystallization despite the highly acidic conditions used[3] highlights the ability of the surfactants to specifically nucleate β-glycine and hinder its solvent-mediated transformation.

A second morphology arising from cellular growth was also obtained from the octanoic acid emulsions stabilized with 8:1 Tween 20/Brij 30. This morphology developed from crystals in which oil droplets were *partially* included, with crystal growth then continuing on either side of the droplets *only* to produce co-aligned dendrites. The co-aligned dendrites often grew rapidly in the *b*-direction initially, since the areas of their (010) faces were too small for strong droplet adhesion. Consequently their porosities were lower. Subsequent lateral growth on these dendrites, though, reduced the mean interdendrite separation and could lead to their subsequent joining in some areas, to produce a highly porous fenestrated structure, see Figure S1b in the Supporting Information.

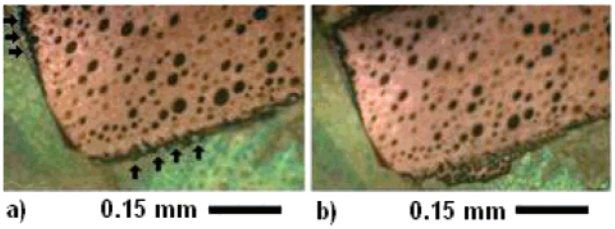

Figure 1. Porous single crystal of β-phase glycine growing from a 60 wt % octanoic acid-in-water emulsion stabilized with 9 wt % of 8:1 Span 20/Brij 30 viewed under crossed polarizers and with a red tint plate to aid crystal distinction. (a) Image taken 23 min after crystallization commenced. Note the highly curved growth fronts (arrowed) due to the adhesion of octanoic acid droplets. Many of these droplets become included in the crystal during subsequent growth, as shown in image (b) which was taken 80 s after image (a).

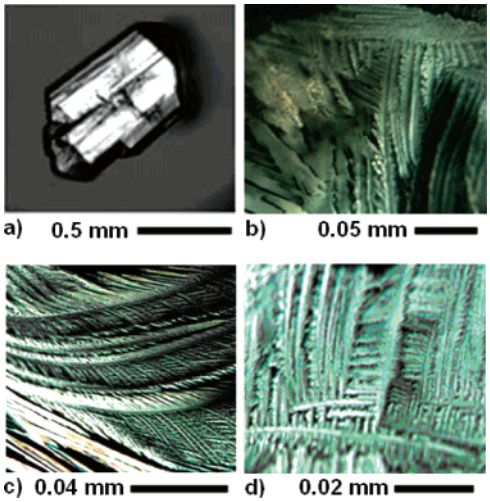

Figure 2. Glycine crystals grown at 20 °C from low supersaturation solutions containing 21.5 wt % glycine viewed under crossed polarizers: (a) normal α-phase morphology obtained from aqueous solution and (b, c, d) β-phase dendritic morphologies achieved in octanoic acid emulsions with a 50 wt % surfactant blend comprising 8:1 Span 20/Brij 30.

On increasing the total surfactant concentration to 50 wt % for the 8:1 Span 20/Brij 30 mix, stable emulsions with smaller octanoic acid droplet sizes of 2−5 μm were obtained. These systems produced a more extreme dendritic morphology for β-glycine, see Figure 2. Initial growth occurred predominantly in the crystallographic *b*-direction, with subsequent dendrites also emerging in the *a*-direction, although 110 growth could also occur occasionally. Further dendritic branching in the *b*- and *a*-directions produced high surface-area crystal morphologies, often with an interwoven appearance. These complex dendritic morphologies are in stark contrast to the facetted crystals that normally develop from aqueous

10.1021/ja0603608 CCC: $33.50

Scheme 1. Development of Porous and Dendritic Crystals through Emulsion Droplet Adhesion

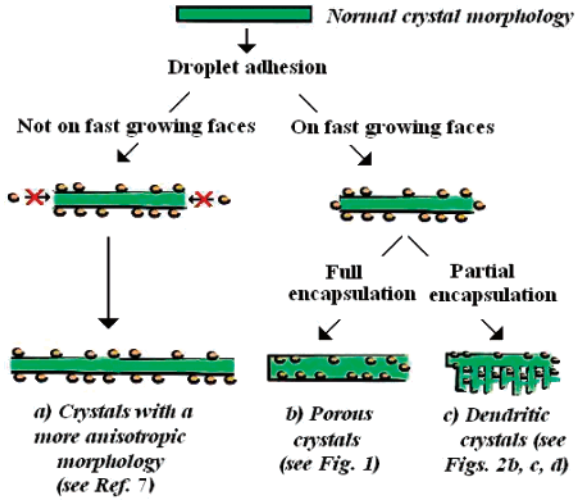

solution at these low supersaturation levels, see Figure 2a. Their occurrence can be attributed to a droplet concentration gradient adjacent to the crystal surface. However, unlike conventional dendritic growth, this concentration gradient arises primarily from the droplet adhesion to the crystal surface, rather than from the crystallization rate proceeding faster than the diffusion of impurity away from the growth front. Hence, when we replace octanoic acid with decane, no dendritic growth occurs, and β-phase needles are obtained. The single-crystal origin of these complex morphologies was evident from the birefringence color continuity and the X-ray diffraction patterns, although the divergence of the dendrite branches often led to a series of closely spaced diffraction spots emanating from diffraction from the same crystallographic plane, rather than a single diffraction spot, see Figure S4, Supporting Information. We believe that the complex dendritic morphologies occur, rather than the macroporous architecture, primarily due to the reduced interfacial activity of the octanoic acid in these high surfactant concentration systems, which decreases the cooperative adhesion between the droplet and crystal surface.[4] However, we do note that smaller droplets require a faster crystal growth for inclusion to occur compared to larger droplets.[5]

These fascinating macroporous and dendritic growth effects are likely to depend on two main factors. First, the octanoic acid must have a relatively high interfacial activity in the emulsions to provide cooperative adhesion via hydrogen bonding to the glycine. We believe this explains why the Span 20 and Tween 20 surfactants promote these unusual morphologies, whereas octanoic acid emulsions stabilized with just Brij 30 produce the needle morphology normally observed for crystals of β-phase glycine.[6] Second, the droplets must adsorb most strongly on the fastest growing faces. This is readily seen in the macroporous crystals by the change in crystal morphology from the typical β-phase needles elongated in the fast-growing *b*-direction to a more platelike morphology as the crystallization and droplet adhesion proceeds. In contrast, selective adsorption on a slower-growing face will merely produce a more asymmetric morphology without droplet inclusion, as in the case of the prismatic-to-needle morphology change observed for L-asparagine monohydrate in octanoic acid emulsions.[7] Whether the resulting morphology provides porous single crystals, fenestrated intergrown crystals, co-aligned dendrites, or complex dendritic forms will then depend on the extent and anisotropy of the crystal growth inhibition. The different mechanisms leading to porous crystal and dendrite development are illustrated in Scheme 1.

The encapsulation of gas bubbles, particularly during melt crystallization, is well-documented; however, few studies have addressed the capture of oil droplets by crystals growing from solution.[5] Moreover, our approach is the first to use emulsion droplets in a dual nucleation promotion/growth inhibition role, enabling control over both the nucleation and growth stages. The use of surfactants and emulsion systems to promote nucleation of specific phases,[8] to induce growth inhibition,[7] and to produce elongated crystals through simultaneous crystallization and droplet dewetting[9] has been reported previously. However, to our knowledge, this is the first time emulsion droplets have been shown to induce such high crystal porosity and intricate single-crystal morphologies. The inclusion of latexes into crystals and the production of complex morphologies using organic molds has recently been reported.[10] Our method has the additional advantage that the emulsion droplets can be removed readily.

In conclusion, we have demonstrated the ability to crystallize the least stable polymorph of glycine and alter its morphology significantly through emulsion droplet adhesion. Partial incorporation of the droplets results in co-aligned dendrites and can produce highly intricate morphologies, whereas porous single crystals are obtained from complete inclusion. Preliminary studies on sodium chloride crystallization from octanoic acid emulsions have shown that similar complex architectures are obtainable, see the Supporting Information. Hence, this methodology may provide a simple, controllable route for production of porous and high surface area, intricate morphology single crystals of many other materials, providing suitable surface-active nucleating agents and adhering cosurfactants can be found.

Acknowledgment. We acknowledge EPSRC for funding for C.E.N. and M.J.J.

Supporting Information Available: Details of the emulsion preparation, crystallization, X-ray diffraction, ESEM and optical microscopy studies; optical micrographs of the co-aligned dendrites and fenestrated morphologies, ESEM images, and typical 2D X-ray diffraction patterns; movies showing the crystal growth and details of the sodium chloride preliminary crystallization studies. This material is available free of charge via the Internet at http://pubs.acs.org.

References

(1) Allen, K.; Davey, R. J.; Ferrari, E.; Towler, C.; Jones, M. O.; Pritchard, R. G. *Cryst. Growth Des.* **2002**, *2*, 523−527.
(2) Ferrari, E. S.; Davey, R. J.; Cross, W. I.; Gillon, A. L.; Towler, C. S. *Cryst. Growth Des.* **2003**, *3*, 53−60.
(3) Towler, C. S.; Davey, R. J.; Lancaster, R. W.; Price, C. J. *J. Am. Chem. Soc.* **2004**, *126*, 13347−13353.
(4) A quantitative analysis of the adhesion energy is beyond the scope of this communication as it will depend on factors such as the disjoining pressure, solution viscosity, and effects of temperature gradients, as well as the difference between the interfacial tension of the crystal−aqueous interface and the crystal−droplet interface. Clearly though, a decrease in the crystal−droplet interfacial tension will promote increased adhesion.
(5) See, e.g., Chernov, A. A.; Temkin, D. E. In *Crystal Growth and Materials*; Kaldis, E., Scheel, H. J., eds.; North-Holland Publishing Company: Amsterdam, 1976; Chapter 1.1.
(6) The use of ~10% Brij 30 in the surfactant mix is advantageous, though, in producing emulsions with less polydispersity in droplet size.
(7) Cooper, S. J. *CrystEngComm* **2001**, art. no. 56.
(8) See, e.g.: (a) Jamieson, M. J.; Nicholson, C. E.; Cooper, S. J. *Cryst. Growth Des.* **2005**, *5*, 451−459. (b) Davey, R. J.; Hilton, A. M.; Garside, J.; de la Fuente, M.; Edmondson, M.; Rainford, P. *J. Chem. Soc., Faraday Trans.* **1996**, *92*, 1927−1933. (c) Kaneko, N.; Horie, T.; Ueno, S.; Yano, J.; Katsuragi, T.; Sato, K. *J. Cryst. Growth* **1999**, *197*, 263−270.
(9) Spicer, P. T.; Hartel, R. W. *Aust. J. Chem.* **2005**, *58*, 655−659.
(10) See: (a) Lu, CH.; Qi, L. M.; Cong, H. L.; Wang, X. Y.; Yang, J. H.; Yang, L. L.; Zhang, D. Y.; Ma, J. M.; Cao, W. X. *Chem. Mater.* **2005**, *17*, 5218−5224. (b) Munoz-Espi, R.; Qi, Y.; Lieberwirth, I.; Gomez, C. M.; Wegner, G. *Chem Eur. J.* **2005**, *12*, 118−129, (c) Yue, W.; Kulak, A. N.; Meldrum, F. C. *J. Mater. Chem.* **2006**, *16*, 408−416.

JA0603608